Abnormal sperm in mice with targeted deletion of the *act* (activator of cAMP-responsive element modulator in testis) gene

Noora Kotaja*†, Dario De Cesare*†‡, Betina Macho*, Lucia Monaco*, Stefano Brancorsini*, Ellen Goossens§, Herman Tournaye§, Anne Gansmuller*, and Paolo Sassone-Corsi*¶

*Institut de Génétique et de Biologie Moléculaire et Cellulaire, B.P. 10142, 67404 Illkirch-Strasbourg, France; and §Centre for Reproductive Medicine, University Hospital, Dutch-Speaking Brussels Free University, Laarbeeklaan 101, B-1090 Brussels, Belgium

Edited by Ryuzo Yanagimachi, University of Hawaii, Honolulu, HI, and approved May 26, 2004 (received for review March 19, 2004)

ACT [activator of cAMP-responsive element modulator (CREM) in testis] is a LIM-only protein that interacts with transcription factor CREM in postmeiotic male germ cells and enhances CREM-dependent transcription. CREM regulates many crucial genes required for spermatid maturation, and targeted mutation of the *Crem* gene in the mouse germ-line blocks spermatogenesis. Here we report the phenotype of mice in which targeted disruption of the *act* gene was obtained by homologous recombination. Whereas the seminiferous tubules of the $act^{-/-}$ mice contain all of the developmental stages of germ cells and the mice are fertile, the amount of mature sperm in the epididymis is drastically reduced. The residual sperm display severe abnormalities, including fully folded tails and aberrant head shapes. These results indicate that numerous postmeiotic genes under CREM control require the coactivator function of ACT. Thus, the fine-tuning of sperm development is achieved by the coordinated action of two transcriptional regulators.

Spermatogenesis is a complex differentiation process leading to the generation of haploid, highly specialized spermatozoa from diploid stem cells. The developmental process begins in the basal compartment of the seminiferous epithelium with spermatogonia that are committed to further differentiation by dividing mitotically to give rise to diploid spermatocytes. Primary spermatocytes undergo two meiotic divisions, resulting in haploid round spermatids. During spermiogenesis, haploid spermatids undergo a complex restructuring program in which most of the cytoplasm is removed, the acrosome and the sperm tail are formed, and the DNA is tightly packed to drastically decrease the nuclear size (1). DNA compaction is achieved by replacing histones with protamines, male germ cell-specific, highly basic chromatin proteins (2). The structure of mature sperm consists of a head and a long flagellum (3). The tail is divided into four distinct segments: the connecting piece adjacent to the head, the midpiece, and the principal and end pieces. The axonema, which contains a central pair of microtubules surrounded by nine outer doublets of microtubules, is located at the center of the flagellum throughout its length. The midpiece contains the tightly packed helical array of mitochondria, and the principal piece is defined by the presence of a fibrous sheath (4). The end piece contains only the axonema. After leaving the testis, spermatozoa further mature during the passage through the epididymal duct. During epididymal maturation, germ cells acquire abilities essential for fertilization, such as forward motility and zona recognition (3).

The complexity of the differentiation process of male germ cells requires a highly specialized program of gene expression. This regulation is achieved by means of unique transcriptional control, chromatin remodeling, and the expression of testis-specific genes or isoforms (5). The *Crem* (cAMP-responsive element modulator) gene encodes the transcriptional activator CREMτ, which is highly expressed in male germ cells (6) and regulates the expression of many important postmeiotic genes, such as the ones encoding protamines and transition proteins (7). Importantly, several postmeiotic genes contain cAMP-response elements in their promoter region. Disruption of the *Crem* gene in mice results in a block of germ-cell development at the first step of spermiogenesis (8, 9), revealing the crucial role of CREM in postmeiotic germ-cell differentiation. CREM is an essential component of a transcriptional complex that includes transcription factor IIA (10) and the testis-specific LIM-only protein ACT (activator of CREM in testis), which functions as a coactivator for CREM (11). ACT is expressed specifically in haploid round and elongating spermatids (11). The subcellular localization of ACT is regulated by the kinesin motor protein, KIF17b, which colocalizes with ACT in haploid spermatids and mediates the transport of ACT from the nucleus to the cytoplasm during spermatid elongation (12). The ACT expression profile fully overlaps with CREM, and the KIF17b-mediated relocalization of ACT to the cytoplasm temporally correlates with the cessation of transcription of CREM-regulated genes (11, 12).

To investigate the role of ACT *in vivo*, we have used gene targeting to generate *act*-null mice by homologous recombination. Although the stages of spermatogenesis seem phenotypically normal, mutant animals display a drastically decreased number of mature germ cells. In addition, a large proportion of the residual mature cells show aberrations in tail and head morphology. These observations indicate that many genes whose function is crucial to the generation of mature germ cells are under the regulatory control of ACT. These genes are likely to represent a subset of the CREM-controlled postmeiotic genes because the primary function of ACT is to operate as a transcriptional coactivator of CREM (11, 13).

Materials and Methods

Generation and Genotyping of Mice. The *act* gene [also denominated *fhl5* (four-and-a-half LIM domains 5) in www.informatics.jax.org] was disrupted by replacing exon II with the neomycin-resistance cassette by using homologous recombination. We injected 129/SvPas embryonic stem-cell clones containing the targeted mutation into C57BL/6 blastocysts. Male chimeras were bred with C57BL/6 mice to obtain germ-line transmission. Heterozygous mice were further bred with 129/SvPas mice. All mice studied here had a mixed genetic background of 25–50% C57BL/6 and 50–75% 129/Sv. DNA was extracted from mice tails by using standard protocols, and genotyping was performed by PCR using specific primers amplifying either the mutant or WT allele. Southern blot analyses of DNA from WT and *act*-null

This paper was submitted directly (Track II) to the PNAS office.

Abbreviations: CREM, cAMP-responsive element modulator; ACT, activator of CREM in testis; FHL, four-and-a-half LIM domains.

†N.K. and D.D.C. contributed equally to this work.

‡Present address: Istituto di Genetica e Biofisica "Adriano Buzzati-Traverso," Via G. Marconi 10, 80125 Naples, Italy.

¶To whom correspondence should be addressed. E-mail: paolosc@igbmc.u-strasbg.fr.

www.pnas.org/cgi/doi/10.1073/pnas.0401947101

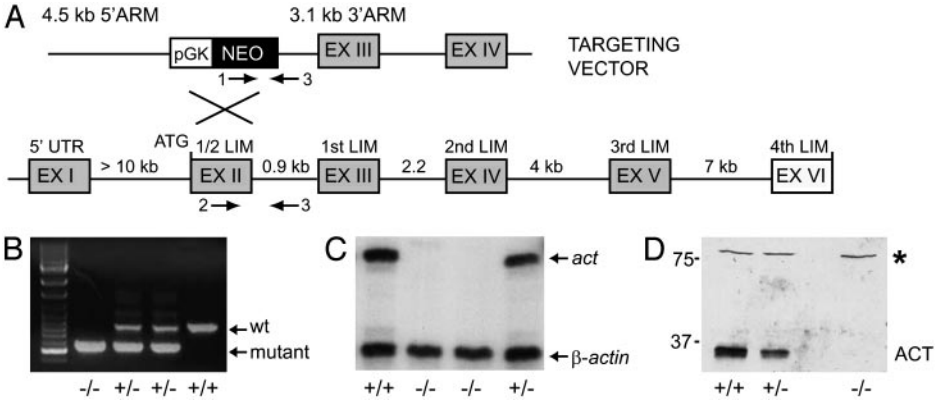

Fig. 1. Targeted disruption of the *act* gene. (*A*) The $act^{-/-}$ knockout mice were generated by disrupting the *act* gene by replacing exon II with a phosphoglycerate kinase–neomycin-resistance cassette. (*B*) The gene disruption was confirmed by PCR genotyping. Tail genomic DNA was amplified with primers specific for the WT (primers 2 and 3; 850 bp) and mutant (primers 1 and 3; 600 bp) *act* allele. (*C*) RNase protection assays demonstrate the lack of ACT transcript in testis RNA of $act^{-/-}$ mice. (*D*) Western blot analysis showing the absence of ACT protein in total testis extracts of $act^{-/-}$ mice. Protein concentrations were measured and Coomassie blue staining was used to verify the equal loading of the samples. The equal intensity of an unspecific protein band recognized by the anti-ACT Ab (*) confirms that equal amounts of total proteins are present in each lane.

clones were performed to confirm correct genomic insertion of the targeting vector and to exclude multiple insertions.

RNA and Protein Analysis. Total RNA was extracted from mouse tissues and analyzed by RNase protection (14). [α-^{32}P]UTP antisense riboprobes were generated by using an *in vitro* transcription kit (Promega). The ACT riboprobe was described in ref. 11. In all RNase protection analyses, transfer RNA was used as a control for nonspecific protection. A mouse β-actin riboprobe was used as internal control to monitor the loading of equal amounts of RNA (fragment from nucleotide +193 to nucleotide +331 of the mouse cDNA). Testis protein extracts for Western blot analysis were prepared as described in ref. 15. Purified rabbit anti-ACT antiserum (1:1,000 dilution) was described in refs. 11 and 13. Horseradish peroxidase-conjugated goat anti-rabbit IgG (Jackson ImmunoResearch) was used as a secondary Ab. Immunocomplexes were detected by enhanced chemiluminescence (Pierce).

Histological Analysis. Freshly dissected testes from +/+ and −/− mice were immersed in Bouins' solution. Sections were prepared according to standard procedures and stained by using hematoxylin/eosin.

Microscopy and Immunocytochemistry. For phase-contrast microscopy, mature sperm were collected from cauda epididymis of *act*-null and WT mice and spread on the glass slides. Samples were air-dried, fixed with 4% paraformaldehyde, and washed in PBS. Some slides were stained with toluidine blue and used for phase-contrast microscopy. Other slides were permeabilized with 0.2% Triton X-100 for 5 min, and nonspecific sites were blocked with 5% BSA for 1 h. The immunofluorescence analysis was performed by using polyclonal K3638 anti-KIF17 Ab (1:200 dilution, Sigma) and Alexa Fluor 594 goat anti-rabbit IgG secondary Ab (Molecular Probes). For electron microscopy, mature spermatozoa from cauda epididymis of the $act^{+/+}$ and $act^{-/-}$ mice were fixed in 2.5% glutaraldehyde and prepared according to standard procedures.

Analysis of Sperm Motility and *in Vitro* Fertilization. Sperm from cauda epididymis of *act*-null and WT males were released in K-modified simplex optimized medium (KSOM) (3% BSA). Sperm motion was assessed by using Computer Assisted Sperm Analysis (HTM-IVOS, Hamilton). For *in vitro* fertilization, sperm were capacitated for 2 h. Six-week-old (C57BL × Cba)F_1 hybrid female mice (Iffa Credo) were induced to superovulate with 5 units of pregnant mare serum gonadotropin (Intervet, Mechelen, Belgium) and, after 48 h, 5 units of human chorionic gonadotropin (Intervet). Sixteen hours after human chorionic gonadotropin injection, eggs were collected from ampullae of oviducts. *In vitro* fertilization was carried out by using standard protocols. Eggs were incubated with 10^5 spermatozoa for 3.5 h at 37°C in KSOM (3% BSA) under mineral oil, and unbound sperm were washed away. After 22-h incubation at 37°C in KSOM (0.5% BSA) under mineral oil, eggs were examined for the presence of the two-cell-stage embryos as an indication of successful fertilization.

Results

Generation of $act^{-/-}$ Mice. To address the functional role of the ACT transcriptional coactivator in male germ cells, we performed targeted disruption of the gene by homologous recombination. We cloned and characterized a genomic fragment containing the mouse *act* gene (Fig. 1*A*), which was used to construct a gene-targeting vector in which the *act* sequence encompassing exon 2 was replaced with a phosphoglycerate kinase–neomycin-resistance cassette (Fig. 1*A*). Exon 2 was chosen for targeting because it contains the ATG codon (11). The targeting vector was introduced into embryonic stem cells by electroporation, and cell clones were isolated and propagated. The targeted embryonic stem-cell clones were microinjected into blastocysts to generate chimeric mice that transmitted the disrupted allele through the germ line. Heterozygous mice were crossed to generate $act^{-/-}$ mice. Genotyping of the mice was performed by PCR using genomic DNA from tails and specific primers recognizing either the WT or mutant allele (Fig. 1*B*). ACT protein is exclusively expressed in germ cells of the seminiferous epithelium (11). RNase protection analysis (Fig. 1*C*) and Western blot analysis using specific anti-ACT Abs (Fig. 1*D*) (11) demonstrated the absence of *act* transcripts and ACT protein in $act^{-/-}$ mice. Heterozygous mice showed reduced levels of expression.

Mice Lacking the *act* Gene Are Fertile. $act^{-/-}$ mice grew normally and showed no obvious anatomical or behavioral defects. Because ACT expression is testis-specific and ACT was shown to cooperate with CREM in transcriptional activation at specific stages of spermatogenesis (11), we wanted to study the testis phenotype of *act*-null animals (8, 9). Fertility of $act^{-/-}$ mice was studied by inducing mating with WT females in estrus. Vaginal plug formation was checked the next morning as an indication of

DEVELOPMENTAL BIOLOGY

successful mating. During the first month of mating, no pregnant females were observed in breeding cages with $act^{-/-}$ males. However, after 1 month, females became pregnant, indicating that *act*-null males were fertile. Statistical analysis after many matings indicated no substantial differences in the ability of WT and *act*-null males to generate offspring in the correct Mendelian frequency. The average litter size in breedings of $act^{-/-}$ mice (9.3 ± 3.7) was not significantly altered as compared with $act^{+/+}$ mice (10.1 ± 2.7).

Drastic Reduction of Mature Sperm in *act*-Null Mice. The important regulatory role of ACT (11, 13) suggested that mutant mice may have abnormalities not affecting fertility. Thus, we investigated in detail the male reproductive organs and the progress of spermatogenesis in the seminiferous epithelium. Testes of $act^{-/-}$ mice appeared normal, although 10% presented a 10–15% reduction in size when compared with WT mice (Fig. 2*A*). Interestingly, the cauda epididymis of *act*-null mice was always smaller and more transparent than WT epididymis, suggesting a reduction in the amount of mature sperm in the epididymal tubules (Fig. 2*B*). Histological paraffin sections of testes stained with hematoxylin and eosin of WT and mutant mice appeared equal (Fig. 2 *C* and *D*). Seminiferous tubules of *act*-null mice contained all of the developmental stages of male germ cells (data not shown). These observations indicate that ACT is not essential for spermatogenesis. To study the properties of mature germ cells, these cells were collected from cauda epididymides of $act^{+/+}$ and $act^{-/-}$ mice to be analyzed. Spermatozoa from epididymides of five WT and mutant mice were counted, and the results indicate that $act^{-/-}$ mice have dramatically lowered sperm counts (Fig. 3*A*) at a level of only 35% of WT mice. Motility and progressivity of sperm were assessed by computer-assisted sperm analysis. Results indicated that mutant spermatozoa were less motile (Fig. 3 *B* and *C*). As predicted from the breeding statistics, we observed no significant differences in the capacity of mutant and WT sperm to fertilize mouse eggs *in vitro* (Fig. 3*D*).

KIF17b Is Present in the Principal Piece of the Sperm Tail. KIF17b belongs to the family of kinesin motor proteins that can use ATP-generated energy to walk along microtubules and carry different cargos (16, 17). KIF17b is testis-specific and was found to interact with ACT in postmeiotic spermatids (12). By means of its ability to determine the intracellular localization of ACT, KIF17b modulates CREM-dependent transcription in germ cells (12). KIF17b was shown to be expressed in round and elongating spermatids (12), and we have found that KIF17b expression levels and intracellular localization are unchanged in ACT-deficient mice (data not shown). In addition, by using indirect immunofluorescence on mature germ cells from the epididymis, we demonstrated that KIF17b is also expressed in mature sperm, being localized mainly in the principal piece of the sperm tail (Fig. 4*A*). This result was obtained by using a specific polyclonal anti-KIF17 Ab and confirmed by peptide-competition assays. No signal was detected in the midpiece of the sperm tail or in the nucleus, whereas the acrosomal region of the sperm head was weakly immunoreactive (data not shown). This observation reveals a previously unrecognized location, and thereby a likely additional function, of KIF17b.

Abnormal Morphology of $act^{-/-}$ Mature Germ Cells. We have analyzed whether the lack of ACT would modify the expression levels and intracellular localization of KIF17b. No apparent differences were detected in round and elongating spermatids of $act^{-/-}$ mice as compared with WT animals (data not shown). Similarly, KIF17b expression levels in the principal piece of the tail appear unchanged (Fig. 4*B*). This analysis, however, allowed us to reveal that most of the sperm tails of the *act*-null mice contained a 180° bend in the principal piece (Fig. 4*B*). Phase-contrast microscopy of mature sperm demonstrated that a large majority of the *act*-null sperm has folded tails (Fig. 4 *C* and *D*). Sperm were counted and the percentage of abnormal tails was calculated. Whereas epididymal sperm from WT mice contains 15% cells with bends in the tail, this percentage is drastically increased to 80% in the $act^{-/-}$ mice (Fig. 4*E*). Heterozygous males displayed a phenotype similar to WT mice. In addition to this defect, we also found that about half of the $act^{-/-}$ mice display an exceptionally high number of spermatozoa with abnormally shaped heads (Fig. 4*F*). We observed several types of aberrant head morphologies. In many cases, the back of the sperm head was malformed with a more angular shape as compared with the smooth round shape of WT mature germ cells. Some of the mutant heads also exhibit a very short apex. Analysis by electron microscopy revealed details of the drastic

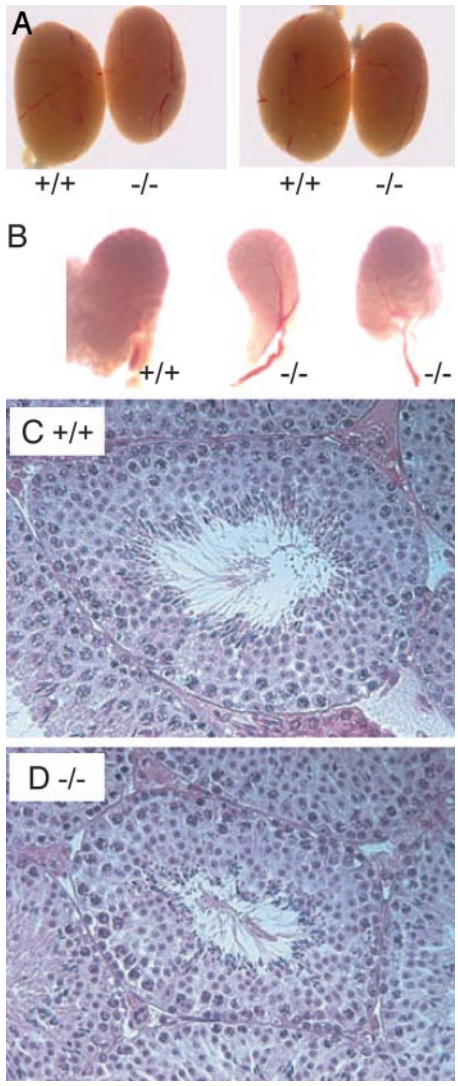

Fig. 2. Testis histology of $act^{-/-}$ mouse is normal. (*A*) No striking differences in testis size between WT and $act^{-/-}$ mice. In some cases, testes of the $-/-$ mice were slightly smaller. (*B*) Cauda epididymides of the $act^{-/-}$ mice are slightly reduced in size and more transparent than those of the WT mice, indicating the reduced amount of mature sperm in the tubules of $-/-$ epididymis. The testis histology of the WT (*C*) and the histology of the mutant (*D*) mice were not significantly different. Testes were fixed in Bouins' solution and embedded in paraffin, and the sections were stained with hematoxylin/eosin. In the seminiferous tubules of $act^{-/-}$ mice, all differentiation stages of male germ cells from spermatogonia to mature sperm were observed. (×50.)

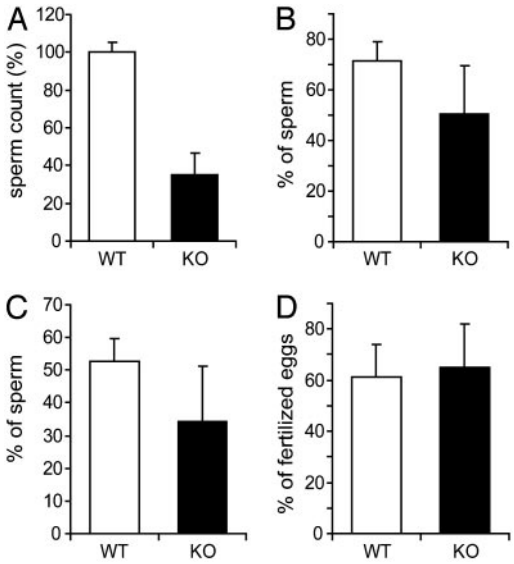

Fig. 3. Reduced sperm counts in the epididymis of ACT-deficient mice. (*A*) Sperm count. Epididymides from WT and $act^{-/-}$ mice were collected, and the sperm was released. The number of sperm in mutant mice (KO) was severely reduced. Motility (*B*) and progressivity (*C*) of the mutant sperm were reduced as assessed by using computer-assisted sperm analysis of the sperm collected from the cauda epididymis. (*D*) The *in vitro* fertilization capacity of the sperm from the *act*-null mice is not significantly changed ($n = 5$ for each genotype). Error bars represent SD.

aberrations of germ cells from the $act^{-/-}$ mice (Fig. 5). Abnormally shaped heads include defects in the compaction of nuclear chromatin and acrosome organization. We observed vacuoles in the nucleus (Fig. 5 *A*, *B*, and *E*), malformations, and detachment of the acrosome (Fig. 5 *B–D*). In some cases, the bend in the tail was adjacent to the nucleus (Fig. 5*E*).

Discussion

The transcriptional regulation of postmeiotic genes follows highly specific rules that seem to be unique to male germ cells (5). CREM has been described as a master switch for numerous postmeiotic genes, and its function involves some components of the general transcription machinery, such as transcription factor IIA (10) and a testis-specific coactivator, ACT (11). Here we have reported the phenotype of mice in which targeted deletion of the *act* gene has been obtained by homologous recombination. In contrast with *Crem*-null mice, which exhibit a complete block of spermiogenesis (8, 9), ACT-deficient mice are able to proceed through the postmeiotic phase and generate mature sperm. Thus, not all postmeiotic CREM-target genes require ACT for their activation. On the other hand, the drastic reduction in the number of mature sperm and the radical abnormalities of the residual cells indicate that ACT is involved in the regulation of numerous essential genes encoding structural components of the mature sperm.

ACT belongs to the family of LIM-only proteins, which includes FHL (four-and-a-half LIM domains) 1, FHL2, FHL3, and FHL4. The expression pattern of FHL proteins is cell-specific, with FHL1 being almost ubiquitous, whereas FHL2 is predominantly expressed in heart, FHL3 in muscle, and FHL4 in testis (13, 18–20). FHL proteins exhibit variable transcriptional activation function and cooperation with numerous nuclear regulators (13, 21–25). Because of the high sequence homology, it is possible that FHL proteins could have redundant functions and that the lack of one could indeed be compensated for by expression or overexpression of another. Yet, the testis-specific FHL4 protein does not interact with CREM and is devoid of

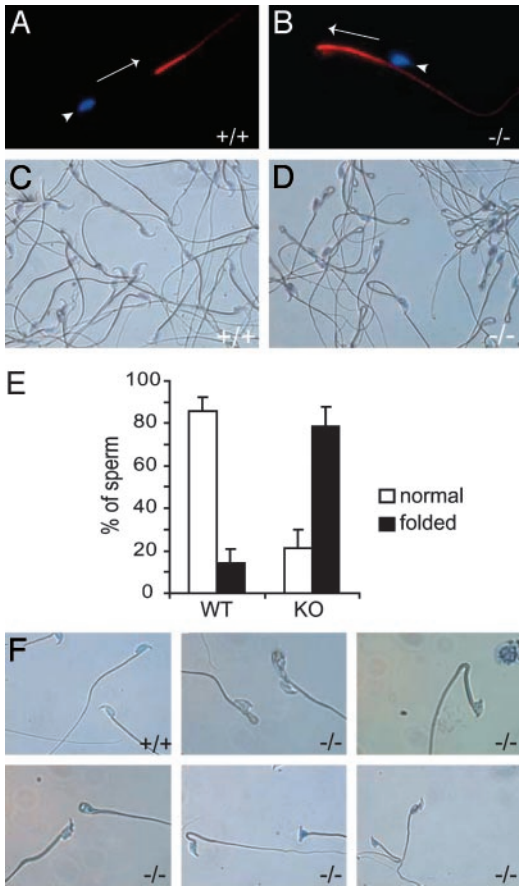

Fig. 4. The $act^{-/-}$ mature spermatozoa have a dramatically increased number of folded tails. (*A* and *B*) Expression of the kinesin protein KIF17b in the mature sperm. KIF17b, which regulates the intracellular localization of ACT in male germ cells, is expressed in the principal piece of the sperm tail in both the WT (*A*) and the $act^{-/-}$ (*B*) mice as detected by immunofluorescence using polyclonal anti-KIF17 Ab and Alexa Fluor 594 anti-rabbit secondary Ab. (×300.) The nuclei are indicated by arrowheads. The position of the unstained midpiece of the sperm tail is indicated by the arrow, which shows the orientation of the tail, pointing toward its tip. (*C* and *D*) Phase-contrast microscopy revealed a much greater number of tail folds in the sperm of $act^{-/-}$ mice. (×150.) Sperm with folded tails were counted. (*E*) The percentages of tail folds compared with total number of counted cells are presented in the graph. (*F*) Examples of abnormally shaped heads of sperm from *act*-null mice. (×300.)

transcriptional activation function in mammalian cells (13). Importantly, the targeted ablation of ACT constitutes a previously unrecognized example of mutation of any FHL protein exhibiting a functional aberration, i.e., mutation of FHL2 in the mouse has no phenotype (26). Interestingly, ACT ablation has no effect on FHL4 expression levels (data not shown).

The abnormally shaped heads and nuclear disorganization present in sperm of $act^{-/-}$ mice reveal defects that could be related to chromatin condensation. Because ACT is not present in mature germ cells (11), a likely scenario is that ACT functions as a coactivator of CREM to regulate the expression of genes that encode architectural components of nuclear chromatin. Thus, the absence of ACT would impair CREM-dependent transcription of these genes or, alternatively, allow CREM to interact with yet-unidentified additional partners, resulting in the control of additional genes. We are not able to support this interesting possibility with experimental data. A survey of the expression of CREM-target genes in the ACT-deficient mice revealed no significant differences, at least in the expression of transition protein 1, protamine-1, and protamine-2 (data not

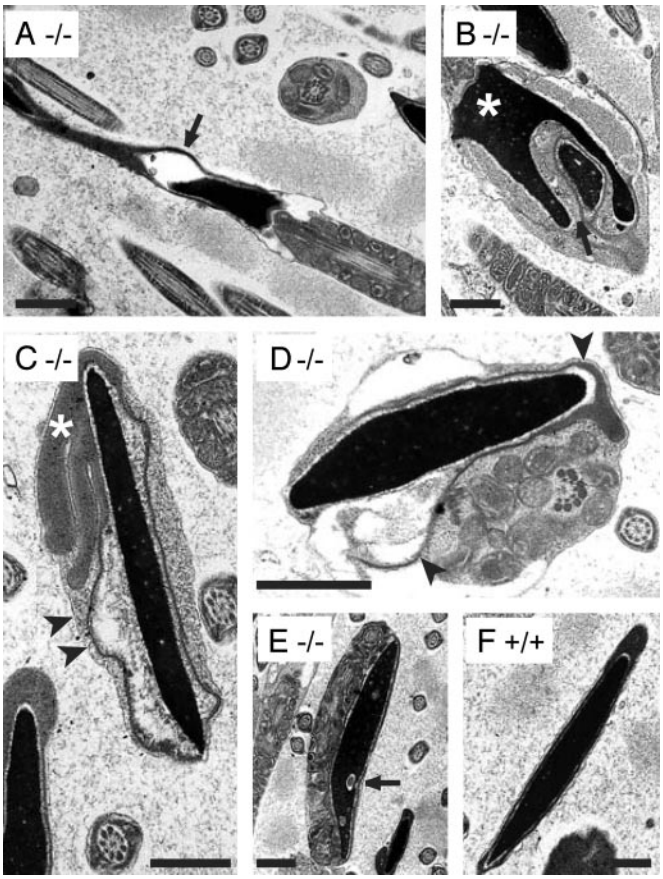

Fig. 5. Electron microscopy of spermatozoa from *act*-null mice. Electron-microscopic analysis of the epididymal sperm revealed many structural abnormalities. In some cells, the nucleus is drastically deformed as shown in *B* (*). Some vacuoles are found inside the nucleus (arrows in *A*, *B*, and *E*). In *C*, the acrosomal malformation with the elongated projections is clearly seen (*). Many sperm cells also have a detached acrosome (arrowheads) (*B–D*). The cross section in *E* also demonstrates the bent tail adjacent to the nucleus. (*F*) Cross section of the nucleus of the WT sperm showing normal acrosome and nuclear shape. (Bar = 0.5 μm.)

shown). An exhaustive analysis by alternative expression profiling would be needed to identify putative CREM–ACT targets. It is also important to note that not all *act*-null mice exhibit abnormalities in the head of sperm. The reason for this variability may be ascribed to different penetrance of the phenotype because of the mixed genetic background of the $act^{-/-}$ mice. Mice lacking the transition protein 2 ($Tnp2^{-/-}$) also show strain-specific features in the phenotype: mutant mice display normal fertility when mated with mixed-background C57BL/6J $\times$ 129/Sv females, but they are infertile when mated with the inbred 129/Sv females (27).

A major abnormality in the epididymal sperm of *act*-null mice is the presence of a high proportion of tails with hairpin loops. ACT is expressed in the nucleus of round spermatids and in the cytoplasm of elongating spermatids, but it is not present in the mature sperm (11, 12). Thus, it is likely that ACT-target genes may include structural proteins that participate in the architectural organization of the flagellum. The formation of the flagellum begins in the cytoplasm of spermatids right after meiosis, when one of the two centrioles at the cell surface forms an axoneme, and continues throughout the spermiogenesis (28). ACT might be needed for the transcription of some components used for the construction of the flagellum during the transcriptionally active phase in round spermatids. In another possible scenario, ACT could be involved in the formation of the tail within the cytoplasm of elongating spermatids, as in this location it was shown to interact with KIF17b, a kinesin motor protein (12). Here we have described the localization of KIF17b also in the principal piece of the mature epididymal sperm (Fig. 4*A*), a location where ACT is absent. This finding points to an interesting connection between ACT and KIF17b and the development of the sperm tail. Lack of ACT could lead to abnormalities in tail development because of the malfunctioning of KIF17b. Additional experiments are needed to address this issue.

Because spermatozoa are highly differentiated and have little cytoplasm except for the membrane-bound droplet on the midpiece, they largely lack the mechanisms necessary for their own osmoregulation and are thus highly dependent on their extracellular environment. The epididymis plays a role in sperm volume regulation. If regulation fails, spermatozoa assume a swollen state, manifested by flagellar coiling or angulation at the site of the cytoplasmic droplet (29). Dysfunction in volume regulation is the cause of infertility in *c-ros* tyrosine kinase-receptor mutant mice, and spermatozoa diluted from the cauda epididymides of these mice were angulated at the midpiece–principal piece junction (30, 31). The susceptibility of flagellar deformation upon swelling changes upon sperm maturation, and sperm from caput epididymis are more susceptible to forming hairpin bends than sperm from cauda epididymis (32). The inability of caudal sperm to bend reflects their stiff flagellum, which resists angulation. Thus, possible explanations for the high percentage of hairpin bends in the tails of $act^{-/-}$ sperm could be structural defects in the sperm tail that allow bending of the flagellum of caudal sperm, but also the failure in the volume regulation of epididymal sperm. It is possible that at least some features of the phenotype could be acquired during storage in the epididymis.

The complex process of spermiogenesis involves a spectacular reshaping of the haploid spermatid cell into a mature spermatozoon. There are a remarkable number and variety of proteins that need to be synthesized to ensure the correct timing in the structuring of the sperm architecture. Our study establishes that ACT, by operating as a coactivator of CREM, plays a role in the late steps of the male germ-cell differentiation program.

We thank Martti Parvinen, Irwin Davidson, Andrée Dierich, and all members of the Sassone-Corsi laboratory for help, reagents, and discussions; and M. Rastegar, S. Roux, E. Heitz, C. Ziegler-Birling, F. Auge, D. Bock, and N. Dondaine for excellent technical assistance and help with the mice. N.K. was supported by a long-term postdoctoral fellowship from the European Molecular Biology Organization and by a grant from Helsingin Sanomain 100-Vuotis Juhlasäätiö (Finland). This work was supported by the Centre National de la Recherche Scientifique, Institut National de la Santé et de la Recherche Médicale, Centre Hospitalier Universitaire Régional, Fondation pour la Recherche Médicale, Université Louis Pasteur, Human Frontier Science Program (RG-240), and Ligue Contre le Cancer.

1. Oakberg, E. F. (1956) *Am. J. Anat.* **99,** 391–413.
2. Ward, W. S. & Coffey, D. S. (1991) *Biol. Reprod.* **44,** 569–574.
3. Toshimori, K. (2003) *Microsc. Res. Tech.* **61,** 1–6.
4. Eddy, E. M., Toshimori, K. & O'Brien, D. A. (2003) *Microsc. Res. Tech.* **61,** 103–115.
5. Sassone-Corsi, P. (2002) *Science* **296,** 2176–2178.
6. Foulkes, N. S., Mellstrom, B., Benusiglio, E. & Sassone-Corsi, P. (1992) *Nature* **355,** 80–84.
7. Sassone-Corsi, P. (1998) *Semin. Cell Dev. Biol.* **9,** 475–482.
8. Nantel, N., Monaco, L., Foulkes, N. S., Masquiller, D., LeMeur, M., Henriksén, K., Dierich, A., Parvinen, M. & Sassone-Corsi, P. (1996) *Nature* **380,** 159–162.
9. Blendy, J. A., Kaestner, K. H., Weinbauer, G. F., Nieschlag, E. & Schutz, G. (1996) *Nature* **380,** 162–165.
10. De Cesare, D., Fimia, G. M., Brancorsini, S., Parvinen, M. & Sassone-Corsi, P. (2003) *Mol. Endocrinol.* **17,** 2554–2565.
11. Fimia, G. M., De Cesare, D. & Sassone-Corsi, P. (1999) *Nature* **398,** 165–169.

12. Macho, B., Brancorsini, S., Fimia, G. M., Setou, M., Hirokawa, N. & Sassone-Corsi, P. (2002) *Science* **298,** 2388–2390.
13. Fimia, G. M., De Cesare, D. & Sassone-Corsi, P. (2000) *Mol. Cell. Biol.* **20,** 8613–8622.
14. Foulkes, N. S., Borrelli, E. & Sassone-Corsi, P. (1991) *Cell* **64,** 739–749.
15. Delmas, V., van der Hoorn, F., Mellstrom, B., Jegou, B. & Sassone-Corsi, P. (1993) *Mol. Endocrinol.* **7,** 1502–1514.
16. Nakagawa, T., Tanaka, Y., Matsuoka, E., Kondo, S., Okada, Y., Noda, Y., Kanai, Y. & Hirokawa, N. (1997) *Proc. Natl. Acad. Sci. USA* **94,** 9654–9659.
17. Miki, H., Setou, M., Kaneshiro, K. & Hirokawa, N. (2001) *Proc. Natl. Acad. Sci. USA* **98,** 7004–7011.
18. Chan, K. K., Tsui, S. K., Lee, S. M., Luk, S. C., Liew, C. C., Fung, K. P., Waye, M. M. & Lee, C. Y. (1998) *Gene* **210,** 345–350.
19. Morgan, M. J. & Madgwick, A. J. A. (1999) *Biochem. Biophys. Res. Commun.* **255,** 251–255.
20. Chu, P.-H., Ruiz-Lozano, P., Zhou, Q., Cai, C. & Chen, J. (2000) *Mech. Dev.* **95,** 259–265.
21. Turner, J., Nicholas, H., Bishop, D., Matthews, J. M. & Crossley, M. (2003) *J. Biol. Chem.* **278,** 12786–12795.
22. Yan, J., Zhu, J., Zhong, H., Lu, Q., Huang, C. & Ye, Q. (2003) *FEBS Lett.* **553,** 183–189.
23. Du, X., Hublitz, P., Gunther, T., Wilhelm, D., Englert, C. & Schule, R. (2002) *Biochim. Biophys. Acta* **1577,** 93–101.
24. Muller, J. M., Isele, U., Metzger, E., Rempel, A., Moser, M., Pscherer, A., Breyer, T., Holubarsch, C., Buettner, R. & Schule, R. (2000) *EMBO J.* **19,** 359–369.
25. Morlon, A. & Sassone-Corsi, P. (2003) *Proc. Natl. Acad. Sci. USA* **100,** 3977–3982.
26. Chu, P. H., Bardwell, W. M., Gu, Y., Ross, J., Jr., & Chen, J. (2000) *Mol. Cell. Biol.* **20,** 7460–7462.
27. Adham, I. M., Nayernia, K., Burkhardt-Göttges, E., Topaloglu, Ö., Dixkens, C., Holstein, A. F. & Engel, W. (2001) *Mol. Hum. Reprod.* **7,** 513–520.
28. Russell, L. D., Ettlin, R. A., Sinha-Hikim, A. P. & Clegg, E. D. (1990) *Histological and Histopathological Evaluation of the Testis* (Cache River Press, St. Louis), pp. 1–40.
29. Cooper, T. G. & Yeung, C.-H. (2003) *Microsc. Res. Tech.* **61,** 28–38.
30. Yeung, C.-H., Sonnenberg-Riethmacher, E. & Cooper, T. G. (1999) *Biol. Reprod.* **61,** 1062–1069.
31. Yeung, C.-H., Wagenfeld, A., Nieschlag, E. & Cooper, T. G. (2000) *Biol. Reprod.* **63,** 612–618.
32. Cooper, T. G. (1986) *Gamete Res.* **14,** 47–56.